

Formation of an impurity band and its quantum confinement in heavily doped GaAs:N

Yong Zhang and A. Mascarenhas

National Renewable Energy Laboratory, Golden, Colorado 80401

H. P. Xin and C. W. Tu

Department of Electrical and Computer Engineering, University of California, San Diego, La Jolla, California 92093

(Received 7 May 1999; revised manuscript received 29 December 1999)

Quantum confinement in GaAs_{1-x}N_x/GaAs quantum wells (0.009 < x < 0.045) is studied using electroreflectance measurements. Formation of an impurity band due to heavy nitrogen doping and the quantum confinement of an electron belonging to such an impurity band have been demonstrated. The formation of an impurity band results in an unusual variation in the electron effective mass with nitrogen doping.

I. INTRODUCTION

Driven by their enormous technological potential for device applications, GaAs_{1-x}N_x, GaInAs_{1-x}N_x and GaP_{1-x}N_x alloys have attracted a great deal of attention in recent years. When compared to conventional alloys, such as GaAs_{1-x}P_x, their electronic properties exhibit an abnormal composition dependence, frequently referred to as “giant band-gap reduction” and “giant bowing.”¹⁻³ A few recent publications^{4,5} have focused on the small- x region of GaAs_{1-x}N_x and GaInAs_{1-x}N_x, where empirical models have been developed to account for the experimentally observed abnormalities: the large band-gap reduction and the nitrogen-activated resonant state. Theoretical calculations have shown that in the dilute-N limit of the alloy the band-edge state is largely localized on N,^{1,3} and that this localization decreases with increasing N.³ A single nitrogen (N) impurity forms a resonant state above the conduction band,⁶ and on increasing the impurity concentration a bound state associated with a particular nitrogen pair complex (NN₁) is observed below the conduction band edge of GaAs, whereas a series of other pair states (NN_{*i*}, $i \geq 3$) are observed just above the conduction band edge.⁷ In a similar system, GaP:N, multiple bound states associated with different pair configurations are observed below the bound state of isolated N at a doping level 1×10^{19} cm⁻³ or higher.⁸⁻¹⁰ On further increasing the N content, a comparable magnitude of the band-gap reduction also occurs for this alloy.^{9,10} The band-gap reduction can be interpreted as resulting from the increased density of states originating from a convolution of the different N pair states which merges with the conduction band minimum of GaP.

From a different viewpoint, if in the very dilute alloy regime one considers GaAsN and GaPN alloys as heavily doped semiconductors, their large band-gap reduction and the associated giant bowing are easier to comprehend. Heavy-doping effects in semiconductors have been studied for decades. At a 0.1% doping level ($\sim 2 \times 10^{19}$ cm⁻³), the band-gap reduction is ~ 100 meV for either n -type Si or n -type GaAs, and this reduction results from impurity band formation.¹¹ For GaAs_{1-x}N_x, it is ~ 50 meV for 0.1% N,⁵ which is not at all surprising. In contrast, 0.1% P doping of GaAs or As doping of GaP causes a negligible change in the band gap. The key factor here is that N introduces bound

states in GaP:N and GaAs:N, but there are no bound states in either GaAs:P or GaP:As. The lowest bound state of the N pair is 143 meV below the fundamental band gap in GaP:N (Ref. 8) and 7 meV in GaAs:N.⁷ Thus, the dilute alloy point of view is more appropriate for systems like GaAs:P or GaP:As which exhibit no giant bowing, whereas the heavy-doping picture is more appropriate for systems like GaAs:N and GaP:N.

In conventional n - or p -type doped semiconductors, heavy doping brings about changes in many characteristics of the semiconductors. Among the characteristics changed are the impurity ionization energy, the fundamental absorption edge, the density of states in the vicinity of the band edges, the energy of the fundamental gap, and the effective mass. Effects causing these changes are the Mott (metal-insulator) transition, the Burstein-Moss shift, band-tailing effects, and band-gap renormalization.¹¹ Some of these effects are not expected in isoelectronic doping, whereas some are common features merely exhibited in a different manner, which makes systems like GaAs:N uniquely different from the more widely studied n - or p -type doped systems.

In this work, we have studied the electronic structure of bulk GaAs_{1-x}N_x and GaAs/GaAs_{1-x}N_x/GaAs quantum wells. In the latter, we shall demonstrate the effects of quantum confinement on the electrons in an impurity band that is a subject of great interest. Such a confinement has rarely been investigated even in conventionally doped systems. By fitting the subband energy levels obtained by electroreflectance measurements, we are able to determine the effective mass and conduction and valence band offsets for GaAs_{1-x}N_x as a function of x at room temperature, and to demonstrate the evolution of the conduction band edge from the heavily doped impurity regime to the dilute alloy regime.

II. SAMPLES AND EXPERIMENTS

Samples were grown by gas-source molecular-beam epitaxy on semi-insulating (100) GaAs substrates. These include five bulk GaAs_{1-x}N_x samples with $x = 0.011, 0.013, 0.017, 0.023,$ and 0.033 , all 1000 Å thick with a 200 Å GaAs cap and a 2500 Å buffer; and six GaAs/GaAs_{1-x}N_x/GaAs multiple quantum well (MQW) structures with the same structure: 70 Å well width, 202 Å barrier thickness, repeated

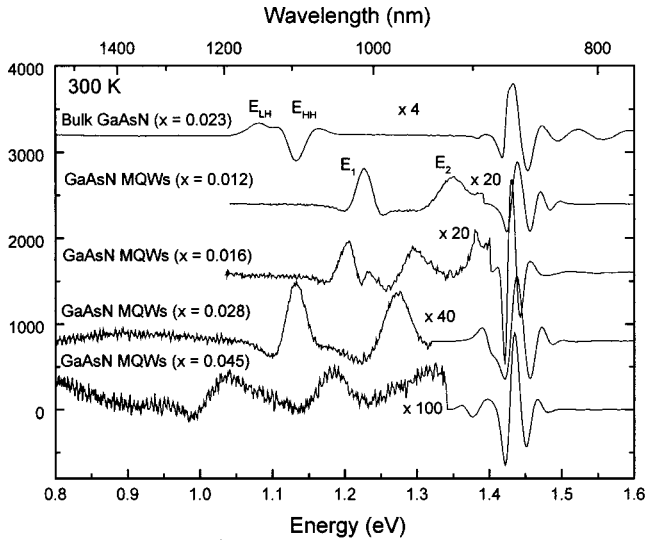


FIG. 1. Electroreflectance spectra for bulk $\text{GaAs}_{1-x}\text{N}_x$ and $\text{GaAs}_{1-x}\text{N}_x/\text{GaAs}$ MQW's.

seven times and capped by a 500 Å GaAs layer. Their x values were 0.009, 0.012, 0.016, 0.020, 0.028, and 0.045, respectively. For the $x=0.016$ MQW structure, a set of four samples were grown with the well width being 30, 50, 70, and 90 Å, respectively. Nitrogen compositions were determined by high-resolution x-ray rocking curve measurements. It has been shown that even for the highest-N composition sample the GaAsN epilayer is still coherently strained by the substrate.^{12,13} Details about the sample growth and the x-ray measurements can be found in a previous publication.¹⁴ Room-temperature electroreflectance spectra were measured using a contactless electroreflectance technique and the experimental setup described in Ref. 5.

III. EXPERIMENTAL RESULTS

Figure 1 shows electroreflectance spectra for a bulk GaAsN and four GaAsN MQW samples. The spectrum for the bulk sample is qualitatively similar to spectra reported previously,¹⁵ except for the fact that the strain-induced valence band splitting is now resolved.¹³ Because the GaAsN layer is under biaxial tensile strain, the topmost valence band is light-hole-like (LH) and the lower band is heavy-hole-like (HH). The higher-energy feature is related to the GaAs cap and buffer, and is not of interest to this study. The transition energies are determined by fitting the spectra to the standard line shape function.¹⁶ Except for the sample with the lowest x , all the 70 Å MQW samples show two transitions below the GaAs band gap, labeled as E_1 and E_2 . For the $x=0.009$ MQW sample, the second transition is in the vicinity of the GaAs feature and so cannot be observed. Transition energies for all the samples are shown in Fig. 2. The quantum confinement effect is apparent, as indicated by the increase in transition energy from that of bulk GaAsN. According to the results of band structure calculations,³ most of the band-gap change occurring from the addition of N results from the lowering of the conduction band edge. Nevertheless, the valence band does move up a little in the region of low N content,³ which means the band alignment between the GaAs and GaAsN is type I. As shown in Fig. 2, until x

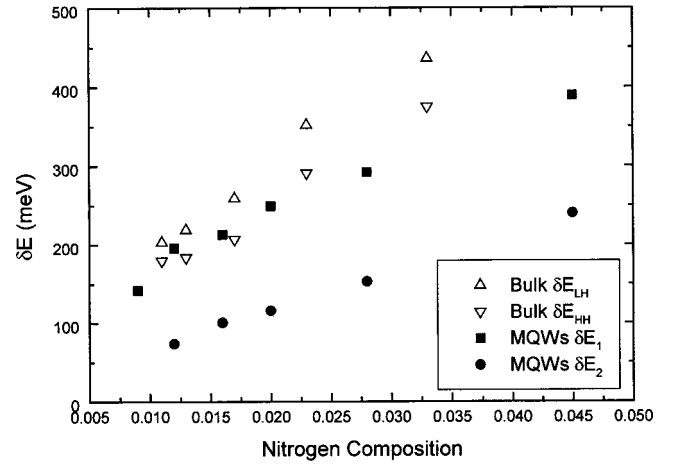


FIG. 2. Transition energies vs nitrogen composition for bulk $\text{GaAs}_{1-x}\text{N}_x$ and $\text{GaAs}_{1-x}\text{N}_x/\text{GaAs}$ MQW's. $\delta E = E_g(\text{GaAs}) - E_g(\text{GaAsN})$.

~ 0.02 , the first intersubband transition energy is below the bulk heavy-hole band edge. Thus, the first transition can only be from the first LH subband to the first conduction subband (LH1 \rightarrow CB1). As for the higher transition, we identify it as the transition LH1 \rightarrow CB3. Other possible assignments could be HH1 \rightarrow CB1 and LH2 \rightarrow CB2. These possibilities can be ruled out, because of the fact that the LH1 and HH1 separation is too small to account for the observed splitting, and the potential well is too shallow to form the second subband for the hole (except for the sample with relatively large x). For $x > 0.02$, the heavy hole becomes confined. Considering the fact that the transition intensity is stronger for the HH state, we attribute the two transitions to HH1 \rightarrow CB1 and HH1 \rightarrow CB3 for $x > 0.02$.

With the experimental values for the band-gap reduction δE_g for bulk GaAsN and the transition energies δE_1 and δE_2 for the QW's, we solve for the conduction band effective mass m^* and the band offset ratio Q_c (defined as $Q_c = \delta E_c / \delta E_g$, where δE_c is the conduction band offset) using a quantum well model with the effective-mass difference between the well and barrier taken into account. We have extrapolated $\delta E_2(x)$ to $x=0.009$. The only assumption that we have to make is that the effective mass of the hole remains the same as that in GaAs ($m_{\text{LH}}=0.09$ and $m_{\text{HH}}=0.377$). Because the N-induced perturbation to the valence band is rather small,³ this assumption should be reasonably sound, at least when x is not too large. We then obtain the composition dependence of the conduction band effective mass, which is shown in Fig. 3 (solid symbols). We acknowledge that there could be some uncertainty in the values of the valence band effective masses in the above analysis. Therefore, we also calculate the electron effective mass by assuming $Q_c=1$ and allowing the barrier height to be a fitting parameter. These results are included in Fig. 3 (open symbols), and can be considered as the upper bound for the electron effective mass.

To further verify our observations, we have studied the dependence of transition energies on well width for a MQW sample with $x=0.016$. Except for the narrowest well (3 nm), two transitions have been observed in the electroreflectance spectra for the other three samples (5, 7, and 9 nm). The

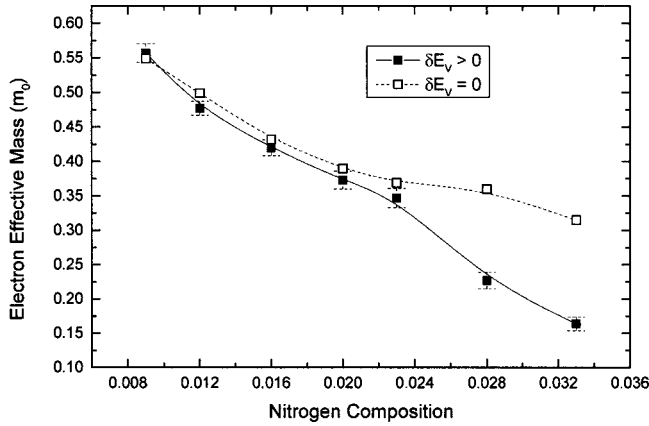


FIG. 3. Electron effective mass of $\text{GaAs}_{1-x}\text{N}_x$ vs the nitrogen composition x .

results are summarized in Fig. 4. Fitting the data to the quantum well model, we get $m_c^* = 0.43$ and $Q_c = 0.83$, which agree very well with the results of $m_c^* = 0.42$ and $Q_c = 0.86$ shown in Fig. 3 that were obtained for the 7 nm quantum well alone.

IV. DISCUSSION

The most significant aspect of the results shown in Fig. 3 is that the effective mass is at first much greater than that for bulk GaAs, and that it is later reduced with further increase in nitrogen doping. In fact, a large conduction band mass has also recently been observed in $\text{GaInAs}_{1-x}\text{N}_x$,¹⁷ but only for one particular composition $x = 0.022$. The results of Fig. 3 are counterintuitive. Based on the $\mathbf{k} \cdot \mathbf{p}$ model, one would expect that the effective mass for dilute GaAs:N should be smaller than that for GaAs because of the band-gap reduction.¹⁵ As will be discussed later, our results provide strong evidence for the formation of an impurity band in GaAsN as the N doping is increased. These results are also consistent with the observation of very low electron mobilities in GaInAsN alloys.¹⁸

In conventional doping of semiconductors, an impurity band starts to form when the doping level reaches $n \sim n_{\text{crit}}$, where n_{crit} refers to the Mott criterion defined as $a_B n_{\text{crit}}^{1/3} = 0.25$ (for GaAs, $n_{\text{crit}} = 1.27 \times 10^{16} \text{ cm}^{-3}$ and $a_B = 103 \text{ \AA}$ is the Bohr radius of the hydrogenlike donor state). On further increasing the doping level, the energy bandwidth increases, and hence the effective mass decreases. For GaAs:N, although the impurity potential of a single N is too weak to generate a bound state, a closely separated N pair does result in a bound state with a binding energy about twice that typical for a donor. Considering each nitrogen pair as an impurity center, the pair concentration can be estimated as $n_{\text{pair}} = m[\text{N}]^2 / (2N_0)$, assuming N atoms are randomly distributed. Here N_0 is the density of the As sites, $[\text{N}]$ is the N concentration, and m is the number of equivalent pair configurations ($m = 12$ for the $[220]$ pairs).⁸ For $x = 0.01$ or $n_{\text{pair}} = 1.3 \times 10^{19} \text{ cm}^{-3}$, the average pair separation $(n_{\text{pair}})^{-1/3}$ is $\sim 42 \text{ \AA}$. The electron binding energy for the pair is $E_b \sim 7 \text{ meV}$, and the electron orbit radius can be estimated using $r = (2m_{\Gamma} E_b / \hbar^2)^{-1/2}$ to be $\sim 63 \text{ \AA}$. Based on this simple consideration, it is not surprising that even below x

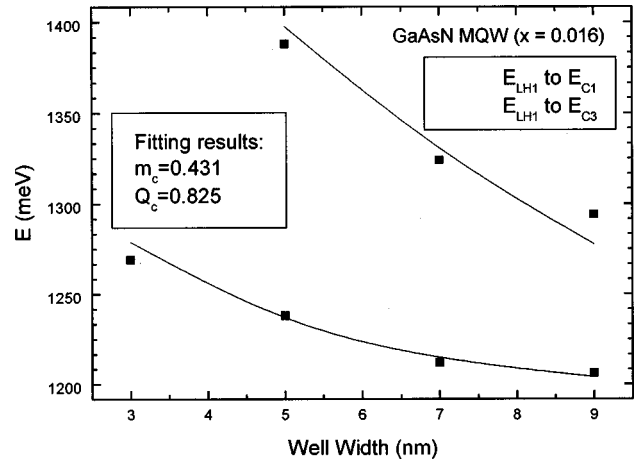


FIG. 4. Transition energies vs quantum well width for $\text{GaAs}_{1-x}\text{N}_x/\text{GaAs}$ MQW's.

$= 0.01$, an impurity band has already formed. For the same doping level, if one compares the present situation to that for donors in GaAs, it is understandable why the band-gap shift is significantly smaller for N doping. This is because (1) the electron orbit radius of the pair state is significantly smaller than the Bohr radius of a typical donor state, and (2) the concentration of the nitrogen pairs is lower than that for the isolated centers. There is, however, a distinct difference between isoelectronic and charged doping. For charged doping, the donor system undergoes a metal-insulator transition at a somewhat higher concentration than n_{crit} , but this kind of transition will never occur in GaAsN. In fact, up to the highest $x = 0.045$, GaAsN behaves like a normal semiconductor.

In Refs. 4, the band-gap reduction and its pressure dependence in GaAsN were explained as being the result of repulsion between the resonant N level and the GaAs band-edge state, which implied that the lower state E_- is GaAs band-edge-like and the higher E_+ is N resonant-state-like. This two-level model has ignored the existence of the N pair bound states observed at relatively low doping levels⁷ and how those levels evolve with increasing N content. The fact is that the pressure dependence of the GaInAsN band gap is rather similar to that of the pair states in either GaAs or GaP,^{7,19} where the pressure behavior (nonlinear and not following any one of the critical points) has been well explained and modeled in terms of the deep impurity properties of N.^{20,21} Another implication of the repulsion model is that the conduction band effective mass will increase with increasing N doping, as a result of the coupling of the GaAs conduction band to the dispersionless N resonant state, which is the opposite of our experimental results. In addition, the model required a delocalized conduction band whereas experiment¹⁸ and theory¹⁻³ indicate the contrary. A modified version of the two-level model was proposed recently.²² In Ref. 22, with the composition dependence of the interband transition matrix element taken into account, the conduction band effective mass was predicted to increase up to $x \sim 0.03$, and subsequently to decrease very slowly, in contrast to the monotonic increase with x predicted by the original two-level model of Ref. 4. Again, the prediction of this modified two-level model does not agree with our experimental results. Two very recent theoretical calculations^{23,24} have shown that the N resonant level interacts more strongly

with the nearby GaAs L points than with the GaAs band-edge Γ point. Thus, we believe that the behavior of the higher-lying isolated nitrogen states does not play a major role in the evolution of the conduction band edge.

We also notice that in GaP:N, at a doping level as high as $1 \times 10^{19} \text{ cm}^{-3}$ ($x \approx 0.04\%$),⁸⁻¹⁰ N atoms still behave like impurities in a semiconductor. Even at a level of $1 \times 10^{20} \text{ cm}^{-3}$ ($x \approx 0.4\%$),^{9,10} one can still see the sharp transition lines from individual nitrogen pairs. In GaAs, formation of the impurity band is evident at a significantly lower doping level $x \sim 0.1\%$. The explanation for this difference in behavior is that the N states are more localized in GaP, because (1) the impurity potential is stronger and (2) the GaP X-point conduction band mass is heavier. Therefore, the critical concentration for impurity band formation is higher in GaP:N. For GaAs:N, a transition from impuritylike to alloylike behavior is expected to occur between $x = 0.01\%$ and $x = 0.1\%$, based on the fact that the linewidth associated with the fundamental band-gap transition as measured in electroreflectance shows a sudden change (a factor of 4) in this region but remains fairly constant elsewhere.⁵ It is within this transition region that the crossover from an increasing to

a decreasing electron effective mass with increasing N doping is expected to occur.

V. CONCLUSIONS

To conclude, we have studied the band structure of bulk GaAsN and GaAsN/GaAs MQW's near the fundamental band gap. Formation of an impurity band due to heavy nitrogen doping and the quantum confinement of an electron belonging to such an impurity band have been demonstrated. By analyzing the subband transitions in the MQW's, we obtain the composition dependence of the conduction band effective mass: the mass, which is at first much larger than that for bulk GaAs, subsequently decreases on further increasing the nitrogen doping, which is precisely what is expected as a result of impurity band formation. We have thus shown that the abnormal conduction band-edge properties of GaAs:N can be easily comprehended by regarding the dilute alloy as a heavily isoelectronic doped semiconductor.

ACKNOWLEDGMENT

This work was supported by the U.S. Department of Energy under Contract No. DE-AC36-83CH10093.

-
- ¹A. Rubio and M. L. Cohen, Phys. Rev. B **51**, 4343 (1995).
²J. Neugebauer and C. G. Van de Walle, Phys. Rev. B **51**, 10 568 (1995).
³S.-H. Wei and A. Zunger, Phys. Rev. Lett. **76**, 664 (1996); L. Bellaiche, S.-H. Wei, and A. Zunger, Phys. Rev. B **54**, 17 568 (1996).
⁴W. Shan, W. Walukiewicz, J. W. Ager III, E. E. Haller, J. F. Geisz, D. J. Friedman, J. M. Olson, and S. R. Kurtz, Phys. Rev. Lett. **82**, 1221 (1999).
⁵J. D. Perkins, A. Mascarenhas, Y. Zhang, J. F. Geisz, D. J. Friedman, J. M. Olson, and S. R. Kurtz, Phys. Rev. Lett. **82**, 3312 (1999).
⁶D. J. Wolford, J. A. Bradley, K. Fry, and J. Thompson, in *Proceedings of the 17th International Conference on the Physics of Semiconductors*, edited by J. D. Chadi and W. A. Harrison (Springer, New York, 1984), p. 627.
⁷X. Liu, M.-E. Pistol, L. Samuelson, S. Schwetlick, and W. Seifert, Appl. Phys. Lett. **56**, 1451 (1990); X. Liu, M.-E. Pistol, and L. Samuelson, Phys. Rev. B **42**, 7504 (1990).
⁸D. G. Thomas and J. J. Hopfield, Phys. Rev. **150**, 680 (1966).
⁹J. N. Baillargeon, K. Y. Cheng, G. E. Hofler, P. J. Pearah, and K. C. Hsieh, Appl. Phys. Lett. **60**, 2540 (1992); X. Liu, S. G. Bishop, J. N. Baillargeon, and K. Y. Cheng, *ibid.* **63**, 208 (1993).
¹⁰H. Yaguchi, S. Miyoshi, G. Biwa, M. Kibune, K. Onabe, Y. Shiraki, and R. Ito, J. Cryst. Growth **170**, 353 (1997).
¹¹E. F. Schubert, *Doping in III-V Semiconductors* (Cambridge University Press, Cambridge, 1993).
¹²K. Uesugi, N. Morooka, and I. Suemune, Appl. Phys. Lett. **74**, 1254 (1999); J. Cryst. Growth **201/202**, 355 (1999).
¹³Y. Zhang, A. Mascarenhas, H. P. Xin, and C. W. Tu, Phys. Rev. B **61**, 7 (2000).
¹⁴H. P. Xin and C. W. Tu, Appl. Phys. Lett. **71**, 2442 (1998).
¹⁵L. Malikova, F. H. Pollak, and R. Bhat, J. Electron. Mater. **27**, 484 (1998).
¹⁶D. E. Aspnes, Surf. Sci. **37**, 418 (1973).
¹⁷E. D. Jones, N. A. Modline, A. A. Allerman, I. J. Fritz, S. R. Kurtz, A. F. Wright, Proc. SPIE **3621**, 52 (1999).
¹⁸J. F. Geisz, D. J. Friedman, J. M. Olson, S. R. Kurtz, and B. M. Keyes, J. Cryst. Growth **195**, 401 (1999).
¹⁹B. Gil, M. Baj, J. Camassel, H. Mathieu, C. Benoit à la Guillaume, N. Mestress, and J. Pascual, Phys. Rev. B **29**, 3398 (1984).
²⁰G. L. Yang, Chin. Phys. Lett. **2**, 197 (1985).
²¹B. Gil, J. P. Albert, J. Camassel, H. Mathieu, and C. Benoit à la Guillaume, Phys. Rev. B **33**, 2701 (1986).
²²A. Lindsay and E. P. O'Reilly, Solid State Commun. **112**, 443 (1999).
²³E. D. Jones, N. A. Modline, A. A. Allerman, S. R. Kurtz, A. F. Wright, S. T. Tozer, and X. Wei, Phys. Rev. B **60**, 4430 (1999).
²⁴T. Mattila, S.-H. Wei, and A. Zunger, Phys. Rev. B **60**, R11 245 (1999).